Dissipationless Spin-Charge Conversion in Excitonic Pseudospin Superfluid

Yeyang Zhang and Ryuichi Shindou*

International Center for Quantum Materials, School of Physics, Peking University, Beijing 100871, China

(Received 31 July 2021; revised 10 December 2021; accepted 18 January 2022; published 8 February 2022)

Spin-charge conversion by the inverse spin Hall effect or inverse Rashba-Edelstein effect is prevalent in spintronics but dissipative. We propose a dissipationless spin-charge conversion mechanism by an excitonic pseudospin superfluid in an electron-hole double-layer system. Magnetic exchange fields lift singlet-triplet degeneracy of interlayer exciton levels in the double-layer system. Condensation of the singlet-triplet hybridized excitons breaks both a U(1) gauge symmetry and a pseudospin rotational symmetry around the fields, leading to spin-charge coupled superflow in the system. We demonstrate the mechanism by deriving spin-charge coupled Josephson equations for the excitonic superflow from a coupled quantum-dot model.

DOI: 10.1103/PhysRevLett.128.066601

Introduction.—Exploring novel approaches to information storage and transport is one of the major challenge in condensed matter physics and quantum information [1–4]. Spintronics utilize spin degree of freedom of electrons [5–10]. As spin voltage or spin current is hardly direct observable, efficient spin-charge conversion becomes a prerequisite for spintronics applications. Inverse spin Hall [11–16] and Rashba-Edelstein [17–23] effects are widely used to convert spin current and spin voltage into charge current, respectively. These effects are accompanied by diffusive quasiparticle transport so that the spin-charge conversions by them are generally lossy.

A dissipationless spin-charge conversion can be realized in superfluids that have both charge [24,25] and spin [26–45] superflow properties. Spin-triplet superconductors [46] and ferromagnetic Josephson junctions [47–52] are among such systems, where spin-polarized Cooper pairs in superconductors are induced by spontaneous symmetry breakings or by magnetic proximity effects [53–57] from ferromagnetic interfaces. In ferromagnetic Josephson junctions, ferromagnetic moments in the interfaces control a relative superconducting phase between spin up and down Cooper pairs, leading to dissipationless Josephson charge and spin currents [48,51]. Nonetheless, the relative phase is a massive mode. Thereby, the finite mass hinders the low-energy conversion from spin voltage to charge current.

Exciton condensates in two-dimensional (2D) electron-hole double-layer (EHDL) systems are ideal platforms for dissipationless conversion between spin voltage and charge current. In the 2D EHDL systems, electron and hole layers are separated from each other by an insulating layer [58–61]. Electrons and holes interact only through Coulomb attraction, which binds them into bound states (excitons). In the presence of a spin-rotational symmetry in either one of the two layers, the bound states have an energy degeneracy between singlet and triplet *excitonic pseudospin* (electrons and holes with opposite spins) levels. Condensation of such excitons breaks not only a relative U(1) gauge symmetry between the two layers but also a pseudospin rotational symmetry, a combination of two spin rotational symmetries in the two layers. The broken gauge symmetry gives rise to electric supercurrents flowing in opposite directions in the two layers [58,62,63], while the broken pseudospin rotational symmetry leads to spin supercurrents. An experimental observation of the charge supercurrents without magnetic field remains illusive at this moment [60,61,64], while it has been observed in the quantum limit [65–72].

In this Letter, we propose a dissipationless spin-charge conversion in the 2D EHDL system under magnetic *exchange fields*. The exchange fields induce a polarization of an excitonic pseudospin. A condensate of such excitons breaks the pseudospin rotational symmetry around the exchange fields and the U(1) gauge symmetry, having two gapless Goldstone modes. We clarify relations among the pseudospin polarization, physical symmetries, and the Goldstone modes in the condensate. We derive spin-charge coupled Josephson equations by a quantum-dot junction model [73,74]. Based on the coupled Josephson equations, we show that a finite static spin voltage (a spatial gradient of the exchange field) leads to an unconventional time-dependent charge supercurrent, giving a microscopic mechanism of the dissipationless spin-charge conversion. We also clarify that spin-orbit coupling (SOC) [75,76] gives rise to spatial textures of the pseudospin polarization in the condensate [77], where the finite static spin voltage induces not only the charge supercurrent but also a dissipationless sliding of the textures.

Model.—The 2D EHDL system (in xy plane) is described by a Hamiltonian ($\hat{H}$):

$$
\begin{aligned}
\hat{K} &\equiv \hat{H} - \mu\hat{N} \\
&= \int d^2\vec{r}\boldsymbol{a}^\dagger(\vec{r})\left[\left(-\frac{\hbar^2\nabla^2}{2m_a} - E_g\right)\boldsymbol{\sigma}_0 + H_a\boldsymbol{\sigma}_x\right]\boldsymbol{a}(\vec{r}) \\
&\quad + \int d^2\vec{r}\boldsymbol{b}^\dagger(\vec{r})\left[\left(\frac{\hbar^2\nabla^2}{2m_b} + E_g\right)\boldsymbol{\sigma}_0 + H_b\boldsymbol{\sigma}_x\right]\boldsymbol{b}(\vec{r}) \\
&\quad + g\sum_{\sigma,\sigma'=\uparrow,\downarrow}\int d^2\vec{r}a_\sigma^\dagger(\vec{r})b_{\sigma'}^\dagger(\vec{r})b_{\sigma'}(\vec{r})a_\sigma(\vec{r}). \qquad (1)
\end{aligned}
$$

Here $\boldsymbol{a} \equiv (a_\uparrow, a_\downarrow)$ and $\boldsymbol{b} \equiv (b_\uparrow, b_\downarrow)$ are annihilation operators of spin-$1/2$ electrons in the electron and hole layer with a positive effective mass m_a and a negative effective mass $-m_b$, respectively. $2E_g$ is an energy difference between the bottom of the electron band and the top of the hole band. Electrons in both layers have chemical potential μ, and $\hat{N}$ is the total number of electrons in the EHDL system. H_a and H_b are magnetic exchange fields in the two layers. The exchange fields can be experimentally induced by the magnetic proximity effect from magnetic substrates. The interlayer interaction is modeled by a short-range interaction with a coupling constant g, while no tunneling between the two layers is allowed. The interaction leads to interlayer s-wave exciton pairing, that can be described by a four-component exciton pairing field $\phi_\mu \equiv (g/2)\langle\boldsymbol{b}^\dagger\boldsymbol{\sigma}_\mu\boldsymbol{a}\rangle$ with pseudospin singlet ($\mu = 0$) and triplet ($\mu = x, y, z$) components. The exchange fields lift fourfold degeneracy of the exciton levels, which causes a singlet-triplet hybridization.

The hybridization can be seen from a ϕ^4-type effective Lagrangian for the four-component exciton pairing field $\vec{\Phi} \equiv (-i\phi_0, \phi_x, \phi_y, \phi_z)$ [77,78] derived from the Hamiltonian [Eq. (1)]:

$$
\begin{aligned}
\mathcal{L} = &-\eta\vec{\Phi}^\dagger\cdot\partial_\tau\vec{\Phi} - \left(\alpha - \frac{2}{g}\right)|\vec{\Phi}|^2 - \gamma[(\vec{\Phi}'^2)^2 + (\vec{\Phi}''^2)^2 \\
&+ 6\vec{\Phi}'^2\vec{\Phi}''^2 - 4(\vec{\Phi}'\cdot\vec{\Phi}'')^2] + \lambda|\nabla\vec{\Phi}|^2 \\
&- 2h(\Phi_y'\Phi_z'' - \Phi_z'\Phi_y'') + 2h'(\Phi_0'\Phi_x'' - \Phi_x'\Phi_0'') + \mathcal{O}(H_{a,b}^2), \qquad (2)
\end{aligned}
$$

where $|\vec{\Phi}|^2 \equiv \vec{\Phi}^\dagger\cdot\vec{\Phi}$ and τ is the imaginary time. Here $\vec{\Phi}'$ and $\vec{\Phi}''$ are real and imaginary parts of the complex-valued four-component exciton field, i.e., $\vec{\Phi} \equiv \vec{\Phi}' + i\vec{\Phi}''$. h and h' are weighted averages between the exchange fields in the electron and hole layers, while their coefficients as well as other parameters (η, α, γ, λ) in the Lagrangian depend on detailed material properties. We assume that $\eta < 0$, $\gamma < 0$, and $\lambda > 0$ [77].

The pseudospin degeneracy is lifted by the h and h' terms (Fig. 1). Energy levels of the singlet-triplet hybridized modes depend on a competition between h and h', which favor $\vec{\Phi}$ polarized within the yz and $0x$ planes, respectively. When a mass of the lowest hybridized mode becomes negative, the excitons undergo condensation. In the condensate phase with finite amplitude of $\vec{\Phi}$, the term $\gamma(\vec{\Phi}'\cdot\vec{\Phi}'')^2$ in the action competes with the exchange terms; the quartic term favors a parallel arrangement of $\vec{\Phi}'$ and $\vec{\Phi}''$, while the two exchange terms favor a perpendicular arrangement. The competition results in a finite angle between $\vec{\Phi}'$ and $\vec{\Phi}''$.

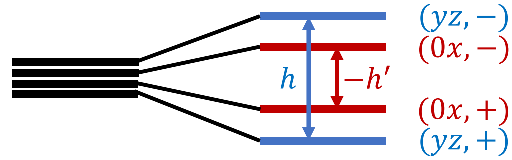

FIG. 1. The fourfold spin degeneracy is lifted by the exchange fields. When $|h| > |h'|$ ($|h| < |h'|$), the lowest band is the transverse (longitudinal) hybrid mode, where the pseudospin polarization is in the yz ($0x$) plane. $(yz/0x, \pm)$ are exciton levels whose pseudospin polarization field $\vec{\phi}$ are in the $yz/0x$ plane, and $\pm$ specifies a relative position between the real and imaginary part of the four-component exciton field $\vec{\phi}$ within the $yz/0x$ plane. The figure is for $h > -h' > 0$.

The nature of the excitonic condensate can be clarified by a minimization of an action $S = \int d\tau d^2\vec{r}\mathcal{L}$ by a τ-independent classical configuration [78]. For $|h| > |h'|$, the action is minimized by a transverse configuration,

$$
\begin{aligned}
\vec{\phi}_\perp(\theta, \varphi, \varphi_0) = &\rho\cos\theta(\cos\varphi_0\vec{e}_y + \sin\varphi_0\vec{e}_z) \\
&+ i\rho\sin\theta[\cos(\varphi + \varphi_0)\vec{e}_y + \sin(\varphi + \varphi_0)\vec{e}_z], \qquad (3)
\end{aligned}
$$

while for $|h| < |h'|$, it is minimized by a longitudinal configuration,

$$
\begin{aligned}
\vec{\phi}_\parallel(\theta, \varphi, \varphi_0) = &\rho[-\sin\theta\cos(\varphi + \varphi_0)\vec{e}_0 + \cos\theta\sin\varphi_0\vec{e}_x] \\
&+ i\rho[\cos\theta\cos\varphi_0\vec{e}_0 + \sin\theta\sin(\varphi + \varphi_0)\vec{e}_x], \qquad (4)
\end{aligned}
$$

with $\rho \equiv \sqrt{h_c/(2|\gamma|)}$ and $h_c \equiv \alpha - 2/g$. Here $\vec{e}_\mu$ ($\mu = 0, x, y, z$) are unit vectors in the four-component vector space. Note also the difference between two coordinate spaces, $\vec{\Phi} \equiv (-i\phi_0, \phi_x, \phi_y, \phi_z)$ and $\vec{\phi} \equiv (\phi_0, \phi_x, \phi_y, \phi_z)$. Equations (3) and (4) are given in the latter coordinate space. φ in the equations is the angle between $\vec{\Phi}'$ and $\vec{\Phi}''$. θ defines a ratio between $|\vec{\Phi}'|$ and $|\vec{\Phi}''|$ through $\tan\theta \equiv |\vec{\Phi}''|/|\vec{\Phi}'|$. φ and θ in Eqs. (3) and (4) form a loop of a minimum-energy degeneracy:

$$
\tilde{h} \equiv \sin\varphi\sin 2\theta = \mathsf{h} \equiv \begin{cases} h/h_c & \text{for } \vec{\phi}_\perp \\ -h'/h_c & \text{for } \vec{\phi}_\parallel. \end{cases} \qquad (5)
$$

We call the exciton condensate with one of these two configurations ("$\perp$" and "$\|$") the transverse (yz) and longitudinal ($0x$) phases, respectively. Both configurations have two arbitrary phase variables. One is φ_0, an overall rotational phase of the pseudospin vector within the yz or $0x$ plane [78]. The other is a combination of θ and φ that satisfies the constraint in Eq. (5). These two are nothing but gapless Goldstone modes associated with broken continuous symmetries. A first-order transition happens at $|h| = |h'| \neq 0$, where the general classical solution is given by a linear superposition of the two configurations [78].

Spontaneously broken symmetries.—Both the yz and $0x$ phases break the relative U(1) gauge symmetry between the two layers. They also break the pseudospin rotational symmetry in which spins in the electron and hole layers are rotated around the field in the same and opposite direction(s), respectively. The two arbitrary phase variables in Eqs. (3)–(5) correspond to the Goldstone modes associated with these symmetry breakings. In fact, they can be absorbed into the relative gauge transformation and the pseudospin rotation by way of a mean-field coupling, $\vec{\phi}_\omega(\theta,\varphi,\varphi_0)\cdot \boldsymbol{a}^\dagger\vec{\boldsymbol{\sigma}}\boldsymbol{b}(\omega=\perp,\|)$. Namely, the coupling is invariant under spin rotations around the x axis together with a change of φ_0 by $\delta\varphi_0$,

$$\begin{gathered}\vec{\phi}_\omega(\theta,\varphi,\varphi_0)\to\vec{\phi}_\omega(\theta,\varphi,\varphi_0+\delta\varphi_0),\\ \boldsymbol{a}\to e^{i\varphi_a\sigma_x}\boldsymbol{a},\qquad \boldsymbol{b}\to e^{i\varphi_b\sigma_x}\boldsymbol{b}=e^{\mp i(\varphi_a+\delta\varphi_0)\sigma_x}\boldsymbol{b}.\end{gathered}\tag{6}$$

Here the "$\mp$" signs in Eq. (6) are for $\omega=\perp,\|$, respectively. The upper and lower signs in "$\pm$" and "$\mp$" in the remainder of this Letter shall be for $\omega=\perp,\|$ respectively. The coupling is also invariant under the relative gauge transformation together with a combination of changes of θ, φ, and φ_0 under the constraint in Eq. (5),

$$\begin{gathered}\vec{\phi}_\omega(\theta,\varphi,\varphi_0)\to e^{i\psi}\vec{\phi}_\omega(\theta,\varphi,\varphi_0)\equiv\vec{\phi}_\omega(\theta(\psi),\varphi(\psi),\varphi_0(\psi)),\\ \boldsymbol{a}\to e^{i\psi_a}\boldsymbol{a},\qquad \boldsymbol{b}\to e^{i\psi_b}\boldsymbol{b}=e^{i(\psi_a-\psi)}\boldsymbol{b}.\end{gathered}\tag{7}$$

Here $(\theta(\psi),\varphi(\psi),\varphi_0(\psi))$ satisfies the constraint in Eq. (5) for an arbitrary U(1) phase ψ. A continuous variation of $(\theta(\psi),\varphi(\psi),\varphi_0(\psi))$ as a function of ψ is shown in Fig. 4 of the Supplemental Material [78]. To emphasize the dependence of $\vec{\phi}_\omega$ on the two variables of the Goldstone modes, we use $\vec{\phi}_\omega(\psi,\tilde{h},\varphi_0)$ instead of $\vec{\phi}_\omega(\theta,\varphi,\varphi_0)$, where $\tilde{h}$ is a massive mode defined in Eq. (5). We further omit $\tilde{h}$ from the arguments of $\vec{\phi}_\omega$ in the following.

Coupled Josephson effects.—As an analogy to pure charge or spin superfluids [26,33], the two Goldstone modes, φ_0 and ψ, are related to spin and charge supercurrents, respectively. Without the exciton condensation, the electron and hole layers have a spin rotational symmetry,

$$\boldsymbol{d}\to e^{i\varphi_d\sigma_x}\boldsymbol{d},\qquad H_d\to H_d-\hbar\partial_t\varphi_d,\tag{8}$$

and a U(1) gauge symmetry,

$$\boldsymbol{d}\to e^{i\psi_d}\boldsymbol{d},\qquad V_d\to V_d-\hbar\partial_t\psi_d,\tag{9}$$

where $\boldsymbol{d}=\boldsymbol{a},\boldsymbol{b}$, and $d=a,b$. V_d and H_d are the electric potential and exchange field along x in the electron ($d=a$) and hole ($d=b$) layer. Spatial differences of $V_d/(-e)$ and $H_d/(-e)$ are defined to be the charge voltage and spin voltage in the electron ($d=a$) and hole ($d=b$) layer, where e is the unit charge. Equations (8) and (9) in combination with Eqs. (6) and (7) suggest that in the excitonic condensate, the charge and spin voltage control the time dependence of ψ and φ_0, respectively. As shown below, the spatial differences of these two gapless phases lead to spin-charge coupled Josephson currents.

The spin-charge coupled Josephson effects can be derived by a quantum-dot junction model [73,78]. The model comprises two domains and a junction between them. Each domain can be regarded as an EHDL quantum dot. The two domains ($j=1,2$) have exciton pairing $\vec{\phi}_\omega(\psi,\varphi_0)$ ($\omega=\perp,\|$) with different values of ψ and φ_0, i.e., ψ_j and φ_{0j} ($j=1,2$). The charge and spin voltages change across the junction in the electron ($d=a$) and hole ($d=b$) layer by V_{Cd} and V_{Sd}, respectively. $e|V_{Sd}|$ is assumed to be much smaller than the exchange fields $|H_d|$, so that variations of the gapped modes (ρ and $\tilde{h}$) can be neglected. An action for the model is given by a functional of V_{Cd}, V_{Sd}, ψ_j, and φ_{0j} ($d=a,b$, $j=1,2$) that takes a quadratic form of the annihilation operators in the electron and hole layers in the two domains, $\boldsymbol{a}_j(\vec{r})$ ($j=1,2$) and $\boldsymbol{b}_j(\vec{r})$ ($j=1,2$). The action is comprised of two parts:

$$\begin{aligned}&\mathcal{S}[\boldsymbol{a}_j,\boldsymbol{a}_j^\dagger,\boldsymbol{b}_j,\boldsymbol{b}_j^\dagger,\psi_j,\varphi_{0j};V_{Cd},V_{Sd}]\\&\quad=\mathcal{S}_T[\boldsymbol{a}_j,\boldsymbol{a}_j^\dagger,\boldsymbol{b}_j,\boldsymbol{b}_j^\dagger]+\mathcal{S}_{\rm mf}[\boldsymbol{a}_j,\boldsymbol{a}_j^\dagger,\boldsymbol{b}_j,\boldsymbol{b}_j^\dagger,\psi_j,\varphi_{0j};V_{Cd},V_{Sd}],\end{aligned}\tag{10}$$

with a mean-field part,

$$\begin{aligned}\mathcal{S}_{\rm mf}=&\int d\tau\sum_{j=1,2}\sum_\alpha\\&\times\bigg\{\boldsymbol{a}_{j\alpha}^\dagger\Big[\hbar\partial_\tau+\boldsymbol{H}_{a\alpha}-\mu-\frac{\eta_j}{2}e(V_{Ca}+V_{Sa}\boldsymbol{\sigma}_x)\Big]\boldsymbol{a}_{j\alpha}\\&+\boldsymbol{b}_{j\alpha}^\dagger\Big[\hbar\partial_\tau+\boldsymbol{H}_{b\alpha}-\mu-\frac{\eta_j}{2}e(V_{Cb}+V_{Sb}\boldsymbol{\sigma}_x)\Big]\boldsymbol{b}_{j\alpha}\\&-[\vec{\phi}_\omega(\psi_j,\varphi_{0j})\cdot\boldsymbol{a}_{j\alpha}^\dagger\vec{\boldsymbol{\sigma}}\boldsymbol{b}_{j\alpha}+\text{H.c.}]\bigg\},\end{aligned}\tag{11}$$

and a tunneling part,

$$\mathcal{S}_T = \int d\tau \sum_{\alpha\beta} [\boldsymbol{a}^\dagger_{1\alpha} T^{(a)}_{\alpha\beta} \boldsymbol{a}_{2\beta} + \boldsymbol{b}^\dagger_{1\alpha} T^{(b)}_{\alpha\beta} \boldsymbol{b}_{2\beta} + \text{H.c.}], \quad (12)$$

with $\eta_1 = -\eta_2 = 1$, $\boldsymbol{a}_j(\vec{r}) \equiv \sum_\alpha u_{aj\alpha}(\vec{r}) \boldsymbol{a}_{j\alpha}$, and $\boldsymbol{b}_j(\vec{r}) \equiv \sum_\alpha u_{bj\alpha}(\vec{r}) \boldsymbol{b}_{j\alpha}$. Here $u_{dj\alpha}(\vec{r})$ is the α-th single-particle eigenstate of the kinetic energy part of Eq. (1) for the electron ($d = a$) and hole ($d = b$) layer in the jth domain region ($j = 1,\ 2$) with a proper boundary condition, together with its eigenenergy $\boldsymbol{H}_{d\alpha} \equiv E_{d\alpha} \boldsymbol{\sigma}_0 + H_d \boldsymbol{\sigma}_x$. Tunneling matrices between the two domains are given by the single-particle eigenstates $T^{(d)}_{\alpha\beta} \equiv \langle u_{d1\alpha} | \mathcal{T}^{(d)} | u_{d2\beta} \rangle$, where $\mathcal{T}^{(d)}$ is the kinetic energy part for the electron ($d = a$) and hole ($d = b$) layer in the junction region. We assume that $\mathcal{T}^{(d)}$ is free from spin or electron-hole mixing.

A perturbative treatment of the tunneling term in the junction model leads to an effective action of the Josephson junction [78]:

$$\begin{aligned} &\mathcal{S}_{\text{eff}}[\tilde{\psi}, \tilde{\varphi}_0, N_C, N_S; V_C, V_S] \\ &= \int d\tau \{ N_C[-i\hbar \dot{\tilde{\psi}}(\tau) - eV_C] + N_S[\mp i\hbar \dot{\tilde{\varphi}}_0(\tau) - eV_S] \\ &- \hbar I_0 \left(\cos\left(\tilde{\psi} - \frac{e}{\hbar c}\Psi\right) \cos\tilde{\varphi}_0 + \bar{h}_\pm \sin\left(\tilde{\psi} - \frac{e}{\hbar c}\Psi\right) \sin\tilde{\varphi}_0 \right) \bigg\}, \end{aligned} \quad (13)$$

with $V_C \equiv V_{Cb} - V_{Ca}$, $V_S \equiv V_{Sb} \pm V_{Sa}$, $\tilde{\varphi}_0 \equiv \varphi_{01} - \varphi_{02}$, $\tilde{\psi} \equiv \psi_1 - \psi_2$, $\dot{\tilde{\varphi}}_0 \equiv \partial_\tau \tilde{\varphi}_0$, and $\dot{\tilde{\psi}} \equiv \partial_\tau \tilde{\psi}$. c is the speed of light. N_C and N_S are differences of total charge and spin between the two domains in the hole layer, respectively [78]. Ψ is an external magnetic flux trapped in the junction region. I_0 and $\bar{h}_\pm$ are constants, and $\bar{h}_\pm$ is proportional to a weighted average of H_a and H_b, while $\bar{h}_+ \neq \bar{h}_-$. Spin currents are defined as differences of charge currents contributed by spin-up and spin-down electrons. By analyses of current directions in the two layers, the currents have relations:

$$\begin{aligned} I_C &\equiv I_{Cb} = -I_{Ca} = e\partial_t N_C, \\ I_S &\equiv I_{Sb} = \pm I_{Sa} = e\partial_t N_S, \end{aligned} \quad (14)$$

where I_{Cd} and I_{Sd} are charge currents and spin currents in the electron ($d = a$) and hole ($d = b$) layer, respectively. Josephson equations can be derived by a minimization of Eq. (13) with Eq. (14) and Wick rotation ($\tau = it$) [78]. The first Josephson equations are

$$\begin{aligned} I_C = -eI_0 \bigg[&\sin\left(\tilde{\psi} - \frac{e}{\hbar c}\Psi\right) \cos\tilde{\varphi}_0 \\ &- \bar{h}_\pm \cos\left(\tilde{\psi} - \frac{e}{\hbar c}\Psi\right) \sin\tilde{\varphi}_0 \bigg], \end{aligned} \quad (15)$$

$$\begin{aligned} \pm I_S = -eI_0 \bigg[&\sin\tilde{\varphi}_0 \cos\left(\tilde{\psi} - \frac{e}{\hbar c}\Psi\right) \\ &- \bar{h}_\pm \cos\tilde{\varphi}_0 \sin\left(\tilde{\psi} - \frac{e}{\hbar c}\Psi\right) \bigg]. \end{aligned} \quad (16)$$

The second Josephson equations are

$$\frac{d\tilde{\psi}}{dt} = -\frac{e}{\hbar} V_C, \qquad \frac{d\tilde{\varphi}_0}{dt} = \mp \frac{e}{\hbar} V_S. \quad (17)$$

The Josephson equations reveal spin-charge coupled Josephson effects. The term proportional to $\sin[\tilde{\psi} - (e/\hbar c)\Psi]$ in Eq. (15) and the term proportional to $\sin(\tilde{\varphi}_0)$ in Eq. (16) represent the well-known pure charge and pure spin Josephson effects [33,79,80], while they are modulated by the spin phase ($\tilde{\varphi}_0$) and the charge phase ($\tilde{\psi}$), respectively. Moreover, the terms proportional to $\bar{h}_\pm$ in Eqs. (15) and (16) indicate that a pure spin (charge) phase difference can still lead to a charge (spin) supercurrent, as the excitons are polarized by the exchange fields. In a multilayer ferromagnetic Josephson junction of superconductors, a relative angle between two ferromagnetic polarizations in two sides of the ferromagnetic junction plays a similar role to the spin phase [48,51]. Unlike the multilayer junction, Eq. (17) further shows control of the spin phase by the spin voltage.

Device setup.—To propose the spin-charge conversion in a feasible experimental setup, we consider putting two magnetic substrates with different magnetizations along the same (x) direction under the hole layer [Fig. 2(a)]. The two substrates introduce the two domains in the EHDL system, whose hole layers experience the magnetic exchange fields through the proximity effect. The difference of the exchange fields results in a finite d.c. spin voltage V_S across the junction in the hole layer. The d.c. spin voltage results in a linear increase of $\tilde{\varphi}_0$, $\tilde{\varphi}_0 = \mp (e/\hbar) V_S t$ ($\tilde{\varphi}_0 = 0$ at $t = 0$ is taken without loss of generality). The time dependence of $\tilde{\varphi}_0$ gives rise to a.c. electric currents in counter-propagating directions in the electron and hole layers, respectively. The electric currents induce the a.c. charge voltages across the junction in the electron and hole layers as $I_{Ca} R_a$ and $I_{Cb} R_b$, where R_a and R_b are external resistances [Fig. 2(a)]. The exciton U(1) phase $\tilde{\psi}$ couples

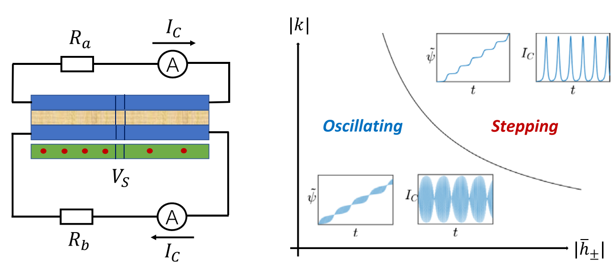

(a) (b)

FIG. 2. The charge current (I_C) induced by the spin voltage (V_S). (a) The spin voltage is added at the Josephson junction in the hole layer. The charge currents can be measured by the two external circuits attached to the electron and hole layers, respectively. (b) The a.c. behavior of $\tilde{\psi}(t)$ and $I_C(t)$ according to Eq. (18) for small $|\bar{h}_\pm|$. $\tilde{\psi}(t)$ shows an oscillating behavior for $|\bar{h}_\pm k| < 1$ and a stepping behavior for $|\bar{h}_\pm k| > 1$.

only with the difference between the charge voltages in the two layers, $V_C = I_{Ca}R_a - I_{Cb}R_b$. Thus, Eqs. (15) and (17) give an equation of motion (EOM) for $\tilde{\psi}$:

$$I_C(s)\frac{R}{V_S} = \frac{d\tilde{\psi}}{ds} = -k[\sin(\tilde{\psi})\cos(s) \pm \bar{h}_{\pm}\cos(\tilde{\psi})\sin(s)], \tag{18}$$

with $R \equiv R_a + R_b$, a normalized time $s \equiv eV_S t/\hbar$, and two dimensionless parameters, $k \equiv eI_0R/V_S$ and $\bar{h}_{\pm}$.

Solutions of the EOM are obtained numerically in the Supplemental Material [78]. $\tilde{\psi}(s)$ shows an oscillating behavior with a double-sine form for $|\bar{h}_{\pm}| < 1/|k|$, and a stepping behaviour for $|\bar{h}_{\pm}| > 1/|k|$ [Fig. 2(b)]. $\tilde{\psi}(s)$ has an oscillatory component with 2π periodicity in s. The $\bar{h}_{\pm}$ term with $\mp k\bar{h}_{\pm} > 0(< 0)$ gives rise to a component of $\tilde{\psi}(s)$ that increases (decreases) linearly in the time s and an additional longer oscillatory periodicity over which $\tilde{\psi}(s)$ increases (decreases) by π. When the longer periodicity approaches the shorter periodicity, the oscillating behavior shows a crossover to the stepping behavior. The double-sine form appears because the electric charge current is induced not only by a sine of the charge phase $\tilde{\psi}$ but also by another sine of the spin phase $\tilde{\varphi}_0$. The spin voltage V_S can be measured from the (short) period of the a.c. electric current [Fig. 2(b)].

Spin-orbit coupling.—A semiconductor heterostructure of the 2D EHDL systems breaks a spatial inversion symmetry, causing an effective Rashba SOC in the electron layer [75,76,81,82]. The Rashba SOC endows the excitonic pseudospin polarizations with a nonzero momentum K in a direction perpendicular to the exchange fields; φ_0 in Eqs. (3) and (4) is replaced by $\varphi_0 - Ky$ [77,78]. The condensate with the broken translational symmetry also has the relative U(1) phase (ψ) and the spin rotational phase (φ_0) as low-energy Goldstone modes. The spin rotational phase φ_0 appears together with the spatial coordinate (y), so that it is also a translational phase (phason). The gapless φ_0 phase originates purely from the spin-rotational symmetry in the hole layer. Charge and (hole-layer) spin voltages control these two gapless modes, respectively [Eq. (17)], while spatial gradients of these two modes generate charge and spin currents as well [78]. Accordingly, the dissipationless spin-charge conversion property is robust against the presence of the Rashba SOC.

Summary.—In this Letter, we clarify the spin-charge coupled Josephson effects in the EHDL exciton system under magnetic exchange fields, where the charge Josephson current can be a response to the spin voltage. The spin-charge coupling effects provide a dissipationless way for the spin-charge conversion in a feasible device setup.

Y. Z. and R. S. thank Junren Shi, Rui-Rui Du, Xi Lin, Ke Chen, Zhenyu Xiao, and Lingxian Kong for their fruitful discussions. The work is supported by the National Basic Research Programs of China (No. 2019YFA0308401) and by the National Natural Science Foundation of China (No. 11674011 and No. 12074008).

*rshindou@pku.edu.cn

[1] M. N. Baibich, J. M. Broto, A. Fert, F. Nguyen Van Dau, F. Petroff, P. Etienne, G. Creuzet, A. Friederich, and J. Chazelas, Giant Magnetoresistance of (001)Fe/(001)Cr Magnetic Superlattices, Phys. Rev. Lett. **61**, 2472 (1988).
[2] G. Binasch, P. Grünberg, F. Saurenbach, and W. Zinn, Enhanced magnetoresistance in layered magnetic structures with antiferromagnetic interlayer exchange, Phys. Rev. B **39**, 4828 (1989).
[3] D. Loss and D. P. DiVincenzo, Quantum computation with quantum dots, Phys. Rev. A **57**, 120 (1998).
[4] I. Žutić, J. Fabian, and S. Das Sarma, Spintronics: Fundamentals and applications, Rev. Mod. Phys. **76**, 323 (2004).
[5] S. K. Kim and Y. Tserkovnyak, Topological Effects on Quantum Phase Slips in Superfluid Spin Transport, Phys. Rev. Lett. **116**, 127201 (2016).
[6] S. K. Kim, S. Takei, and Y. Tserkovnyak, Thermally activated phase slips in superfluid spin transport in magnetic wires, Phys. Rev. B **93**, 020402(R) (2016).
[7] Y. Tserkovnyak, Perspective: (Beyond) spin transport in insulators, J. Appl. Phys. **124**, 190901 (2018).
[8] Y. Tserkovnyak and J. Zou, Quantum hydrodynamics of vorticity, Phys. Rev. Research **1**, 033071 (2019).
[9] J. Zou, S. K. Kim, and Y. Tserkovnyak, Topological transport of vorticity in Heisenberg magnets, Phys. Rev. B **99**, 180402(R) (2019).
[10] S. Dasgupta, S. Zhang, I. Bah, and O. Tchernyshyov, Quantum Statistics of Vortices from a Dual Theory of the *XY* Ferromagnet, Phys. Rev. Lett. **124**, 157203 (2020).
[11] E. Saitoh, M. Ueda, H. Miyajima, and G. Tatara, Conversion of spin current into charge current at room temperature: Inverse spin-Hall effect, Appl. Phys. Lett. **88**, 182509 (2006).
[12] M. V. Costache, M. Sladkov, S. M. Watts, C. H. van der Wal, and B. J. van Wees, Electrical Detection of Spin Pumping Due to the Precessing Magnetization of a Single Ferromagnet, Phys. Rev. Lett. **97**, 216603 (2006).
[13] T. Kimura, Y. Otani, T. Sato, S. Takahashi, and S. Maekawa, Room-Temperature Reversible Spin Hall Effect, Phys. Rev. Lett. **98**, 156601 (2007).
[14] S. Takei and Y. Tserkovnyak, Nonlocal Magnetoresistance Mediated by Spin Superfluidity, Phys. Rev. Lett. **115**, 156604 (2015).
[15] L. J. Cornelissen, J. Liu, R. A. Duine, J. B. Youssef, and B. J. van Wees, Long-distance transport of magnon spin information in a magnetic insulator at room temperature, Nat. Phys. **11**, 1022 (2015).
[16] W. Yuan, Q. Zhu, T. Su, Y. Yao, W. Xing, Y. Chen, Y. Ma, X. Lin, J. Shi, R. Shindou, X. C. Xie, and W. Han, Experimental signatures of spin superfluid ground state in

canted antiferromagnet Cr_2O_3 via nonlocal spin transport, Sci. Adv. **4**, eaat1098 (2018).

[17] J. C. R. Sánchez, L. Vila, G. Desfonds, S. Gambarelli, J. P. Attané, J. M. D. Teresa, C. Magén, and A. Fert, Spin-to-charge conversion using Rashba coupling at the interface between non-magnetic materials, Nat. Commun. **4**, 2944 (2013).

[18] K. Shen, G. Vignale, and R. Raimondi, Microscopic Theory of the Inverse Edelstein Effect, Phys. Rev. Lett. **112**, 096601 (2014).

[19] W. Zhang, M. B. Jungfleisch, W. Jiang, J. E. Pearson, and A. Hoffmann, Spin pumping and inverse Rashba-Edelstein effect in NiFe/Ag/Bi and NiFe/Ag/Sb, J. Appl. Phys. **117**, 17C727 (2015).

[20] J.-C. Rojas-Sánchez, S. Oyarzún, Y. Fu, A. Marty, C. Vergnaud, S. Gambarelli, L. Vila, M. Jamet, Y. Ohtsubo, A. Taleb-Ibrahimi, P. Le Fèvre, F. Bertran, N. Reyren, J.-M. George, and A. Fert, Spin to Charge Conversion at Room Temperature by Spin Pumping into a New Type of Topological Insulator: α-Sn Films, Phys. Rev. Lett. **116**, 096602 (2016).

[21] E. Lesne, Y. Fu, S. Oyarzun, J. C. Rojas-Sánchez, D. C. Vaz, H. Naganuma, G. Sicoli, J.-P. Attané, M. Jamet, E. Jacquet, J.-M. George, A. Barthélémy, H. Jaffrès, A. Fert, M. Bibes, and L. Vila, Highly efficient and tunable spin-to-charge conversion through Rashba coupling at oxide interfaces, Nat. Mater. **15**, 1261 (2016).

[22] M. Isasa, M. C. Martínez-Velarte, E. Villamor, C. Magén, L. Morellón, J. M. De Teresa, M. R. Ibarra, G. Vignale, E. V. Chulkov, E. E. Krasovskii, L. E. Hueso, and F. Casanova, Origin of inverse Rashba-Edelstein effect detected at the Cu/Bi interface using lateral spin valves, Phys. Rev. B **93**, 014420 (2016).

[23] Q. Song, H. Zhang, T. Su, W. Yuan, Y. Chen, W. Xing, J. Shi, J. Sun, and W. Han, Observation of inverse Edelstein effect in Rashba-split 2DEG between $SrTiO_3$ and $LaAlO_3$ at room temperature, Sci. Adv. **3**, e1602312 (2017).

[24] J. Bardeen, L. N. Cooper, and J. R. Schrieffer, Theory of superconductivity, Phys. Rev. **108**, 1175 (1957).

[25] J. G. Bednorz and K. A. Müller, Possible high T_c superconductivity in the Ba-La-Cu-O system, Z. Phys. B Condens. Matter **64**, 189 (1986).

[26] G. E. Volovik, *The Universe in a Helium Droplet* (Clarendon Press, Oxford, 2003).

[27] B. I. Halperin and T. M. Rice, Possible anomalies at a semimetal-semiconductor transistion, Rev. Mod. Phys. **40**, 755 (1968).

[28] E. Sonin, Phase fixation, excitonic and spin superfluidity of electron-hole pairs and antiferromagnetic chromium, Solid State Commun. **25**, 253 (1978).

[29] E. B. Sonin, Analogs of superfluid flows for spins and electron-hole pairs, Sov. Phys. JETP **47**, 1091 (1978) [Zh. Eksp. Teor. Fiz. **74**, 2097 (1978)].

[30] J. König, M. C. Bønsager, and A. H. MacDonald, Dissipationless Spin Transport in Thin Film Ferromagnets, Phys. Rev. Lett. **87**, 187202 (2001).

[31] T. Hakioğlu and M. Şahin, Excitonic Condensation under Spin-Orbit Coupling and BEC-BCS Crossover, Phys. Rev. Lett. **98**, 166405 (2007).

[32] M. A. Can and T. Hakioğlu, Unconventional Pairing in Excitonic Condensates under Spin-Orbit Coupling, Phys. Rev. Lett. **103**, 086404 (2009).

[33] E. Sonin, Spin currents and spin superfluidity, Adv. Phys. **59**, 181 (2010).

[34] Q.-F. Sun, Z.-T. Jiang, Y. Yu, and X. C. Xie, Spin superconductor in ferromagnetic graphene, Phys. Rev. B **84**, 214501 (2011).

[35] S. A. Bender, R. A. Duine, and Y. Tserkovnyak, Electronic Pumping of Quasiequilibrium Bose-Einstein-Condensed Magnons, Phys. Rev. Lett. **108**, 246601 (2012).

[36] Q.-F. Sun and X. C. Xie, Spin-polarized $\nu = 0$ state of graphene: A spin superconductor, Phys. Rev. B **87**, 245427 (2013).

[37] S. Takei and Y. Tserkovnyak, Superfluid Spin Transport through Easy-Plane Ferromagnetic Insulators, Phys. Rev. Lett. **112**, 227201 (2014).

[38] S. Takei, B. I. Halperin, A. Yacoby, and Y. Tserkovnyak, Superfluid spin transport through antiferromagnetic insulators, Phys. Rev. B **90**, 094408 (2014).

[39] H. Chen, A. D. Kent, A. H. MacDonald, and I. Sodemann, Nonlocal transport mediated by spin supercurrents, Phys. Rev. B **90**, 220401(R) (2014).

[40] K. Nakata, K. A. van Hoogdalem, P. Simon, and D. Loss, Josephson and persistent spin currents in Bose-Einstein condensates of magnons, Phys. Rev. B **90**, 144419 (2014).

[41] S. Hoffman and Y. Tserkovnyak, Magnetic exchange and nonequilibrium spin current through interacting quantum dots, Phys. Rev. B **91**, 245427 (2015).

[42] R. A. Duine, A. Brataas, S. A. Bender, and Y. Tserkovnyak, Spintronics and magnon Bose-Einstein condensation, arXiv:1505.01329.

[43] S. Takei, A. Yacoby, B. I. Halperin, and Y. Tserkovnyak, Spin Superfluidity in the $\nu = 0$ Quantum Hall State of Graphene, Phys. Rev. Lett. **116**, 216801 (2016).

[44] Y. Liu, G. Yin, J. Zang, R. K. Lake, and Y. Barlas, Spin-Josephson effects in exchange coupled antiferromagnetic insulators, Phys. Rev. B **94**, 094434 (2016).

[45] S. B. Chung, S. K. Kim, K. H. Lee, and Y. Tserkovnyak, Cooper-Pair Spin Current in a Strontium Ruthenate Heterostructure, Phys. Rev. Lett. **121**, 167001 (2018).

[46] M. Sigrist and K. Ueda, Phenomenological theory of unconventional superconductivity, Rev. Mod. Phys. **63**, 239 (1991).

[47] X. Waintal and P. W. Brouwer, Magnetic exchange interaction induced by a Josephson current, Phys. Rev. B **65**, 054407 (2002).

[48] R. Grein, M. Eschrig, G. Metalidis, and G. Schön, Spin-Dependent Cooper Pair Phase and Pure Spin Supercurrents in Strongly Polarized Ferromagnets, Phys. Rev. Lett. **102**, 227005 (2009).

[49] K. Halterman and M. Alidoust, Josephson currents and spin-transfer torques in ballistic SFSFS nanojunctions, Supercond. Sci. Technol. **29**, 055007 (2016).

[50] M. Eschrig, Spin-polarized supercurrents for spintronics, Phys. Today **64**, No. 1, 43 (2011).

[51] M. Eschrig, Spin-polarized supercurrents for spintronics: A review of current progress, Rep. Prog. Phys. **78**, 104501 (2015).

[52] J. Linder and J. W. A. Robinson, Superconducting spintronics, Nat. Phys. **11**, 307 (2015).

[53] T. Tokuyasu, J. A. Sauls, and D. Rainer, Proximity effect of a ferromagnetic insulator in contact with a superconductor, Phys. Rev. B **38**, 8823 (1988).

[54] A. I. Buzdin, Proximity effects in superconductor-ferromagnet heterostructures, Rev. Mod. Phys. **77**, 935 (2005).

[55] F. S. Bergeret, A. F. Volkov, and K. B. Efetov, Odd triplet superconductivity and related phenomena in superconductor-ferromagnet structures, Rev. Mod. Phys. **77**, 1321 (2005).

[56] K. Ohnishi, S. Komori, G. Yang, K.-R. Jeon, L. A. B. O. Olthof, X. Montiel, M. G. Blamire, and J. W. A. Robinson, Spin-transport in superconductors, Appl. Phys. Lett. **116**, 130501 (2020).

[57] R. Cai, Y. Yao, P. Lv, Y. Ma, W. Xing, B. Li, Y. Ji, H. Zhou, C. Shen, S. Jia, X. C. Xie, I. Žutić, Q.-F. Sun, and W. Han, Evidence for anisotropic spin-triplet Andreev reflection at the 2D van der Waals ferromagnet/superconductor interface, Nat. Commun. **12**, 6725 (2021).

[58] X. Zhu, P. B. Littlewood, M. S. Hybertsen, and T. M. Rice, Exciton Condensate in Semiconductor Quantum Well Structures, Phys. Rev. Lett. **74**, 1633 (1995).

[59] Y. Naveh and B. Laikhtman, Excitonic Instability and Electric-Field-Induced Phase Transition Towards a Two-Dimensional Exciton Condensate, Phys. Rev. Lett. **77**, 900 (1996).

[60] X. Wu, W. Lou, K. Chang, G. Sullivan, and R.-R. Du, Resistive signature of excitonic coupling in an electron-hole double layer with a middle barrier, Phys. Rev. B **99**, 085307 (2019).

[61] X.-J. Wu, W. Lou, K. Chang, G. Sullivan, A. Ikhlassi, and R.-R. Du, Electrically tuning many-body states in a Coulomb-coupled InAs/InGaSb double layer, Phys. Rev. B **100**, 165309 (2019).

[62] Y. E. Lozovik and V. I. Yudson, Feasibility of superfluidity of paired spatially separated electrons and holes; a new superconductivity mechanism, JETP Lett. **22**, 274 (1975).

[63] J. P. Eisenstein and A. H. MacDonald, Bose–Einstein condensation of excitons in bilayer electron systems, Nature (London) **432**, 691 (2004).

[64] G. W. Burg, N. Prasad, K. Kim, T. Taniguchi, K. Watanabe, A. H. MacDonald, L. F. Register, and E. Tutuc, Strongly Enhanced Tunneling at Total Charge Neutrality in Double-Bilayer Graphene-WSe_2 Heterostructures, Phys. Rev. Lett. **120**, 177702 (2018).

[65] I. B. Spielman, J. P. Eisenstein, L. N. Pfeiffer, and K. W. West, Resonantly Enhanced Tunneling in a Double Layer Quantum Hall Ferromagnet, Phys. Rev. Lett. **84**, 5808 (2000).

[66] E. Tutuc, M. Shayegan, and D. A. Huse, Counterflow Measurements in Strongly Correlated GaAs Hole Bilayers: Evidence for Electron-Hole Pairing, Phys. Rev. Lett. **93**, 036802 (2004).

[67] M. Kellogg, J. P. Eisenstein, L. N. Pfeiffer, and K. W. West, Vanishing Hall Resistance at High Magnetic Field in a Double-Layer Two-Dimensional Electron System, Phys. Rev. Lett. **93**, 036801 (2004).

[68] R. D. Wiersma, J. G. S. Lok, S. Kraus, W. Dietsche, K. von Klitzing, D. Schuh, M. Bichler, H.-P. Tranitz, and W. Wegscheider, Activated Transport in the Separate Layers that Form the $\nu_T = 1$ Exciton Condensate, Phys. Rev. Lett. **93**, 266805 (2004).

[69] Y. Yoon, L. Tiemann, S. Schmult, W. Dietsche, K. von Klitzing, and W. Wegscheider, Interlayer Tunneling in Counterflow Experiments on the Excitonic Condensate in Quantum Hall Bilayers, Phys. Rev. Lett. **104**, 116802 (2010).

[70] D. Nandi, A. D. K. Finck, J. P. Eisenstein, L. N. Pfeiffer, and K. W. West, Exciton condensation and perfect Coulomb drag, Nature (London) **488**, 481 (2012).

[71] X. Liu, K. Watanabe, T. Taniguchi, B. I. Halperin, and P. Kim, Quantum Hall drag of exciton condensate in graphene, Nat. Phys. **13**, 746 (2017).

[72] J. I. A. Li, T. Taniguchi, K. Watanabe, J. Hone, and C. R. Dean, Excitonic superfluid phase in double bilayer graphene, Nat. Phys. **13**, 751 (2017).

[73] A. Altland B. D. Simons, *Condensed Matter Field Theory* (Cambridge University Press, Cambridge, London, 2010).

[74] U. Eckern, G. Schön, and V. Ambegaokar, Quantum dynamics of a superconducting tunnel junction, Phys. Rev. B **30**, 6419 (1984).

[75] R. Winkler, *Spin-Orbit Coupling Effects in Two-Dimensional Electron and Hole Systems* (Springer, Heidelberg, 2003).

[76] C. Liu, T. L. Hughes, X.-L. Qi, K. Wang, and S.-C. Zhang, Quantum Spin Hall Effect in Inverted Type-II Semiconductors, Phys. Rev. Lett. **100**, 236601 (2008).

[77] K. Chen and R. Shindou, Helicoidal excitonic phase in an electron-hole double-layer system, Phys. Rev. B **100**, 035130 (2019).

[78] See Supplemental Material at http://link.aps.org/supplemental/10.1103/PhysRevLett.128.066601 for derivations of ϕ^4-type effective Lagrangian, classical-ground states with and without Rashba SOC, relations between Goldstone modes and symmetry breaking in the excitonic condensate phases, spin-charge coupled Josephson equations with and without Rashba SOC, and numerical solutions of the spin-charge coupled Josephson equations.

[79] B. D. Josephson, The discovery of tunnelling supercurrents, Rev. Mod. Phys. **46**, 251 (1974).

[80] S. Takei, Y. Tserkovnyak, and M. Mohseni, Spin superfluid Josephson quantum devices, Phys. Rev. B **95**, 144402 (2017).

[81] C.-X. Liu, X.-L. Qi, H. J. Zhang, X. Dai, Z. Fang, and S.-C. Zhang, Model Hamiltonian for topological insulators, Phys. Rev. B **82**, 045122 (2010).

[82] D. I. Pikulin and T. Hyart, Interplay of Exciton Condensation and the Quantum Spin Hall Effect in InAs/GaSb Bilayers, Phys. Rev. Lett. **112**, 176403 (2014).